Neuroprotective brain-derived neurotrophic factor signaling in the TAU-P301L tauopathy zebrafish model

Clément Barbereau, Alaa Yehya, Michelle Silhol, Nicolas Cubedo, Jean-Michel Verdier, Tangui Maurice, Mireille Rossel

Neuroprotective Brain-Derived Neurotrophic Factor signaling in the TAU-P301L tauopathy zebrafish model

Clément Barbereau*, Alaa Yehya*, Michelle Silhol, Nicolas Cubedo, Jean-Michel Verdier, Tangui Maurice and Mireille Rossel

[1]MMDN, Univ. Montpellier, EPHE, INSERM, U1198, PSL Research University, Montpellier, F-34095 France

* CB and AY contributed equally to the study

Corresponding author:

Mireille ROSSEL

Molecular Mechanisms of Neurodegenerative Dementia

INSERM U1198 - UM - EPHE

CC 105, Place Eugène Bataillon, 34095 Montpellier cedex 5, France

Tel.: 33 4 67 14 38 15. Email address: mireille.rossel@umontpellier.fr

Abstract

Brain–derived neurotrophic factor (BDNF) dysregulations contribute to the neurotoxicity in neurodegenerative pathologies and could be efficiently targeted by therapies. In Alzheimer's disease (AD), although the relationship between BDNF and amyloid load has been extensively studied, how Tau pathology affects BDNF signaling remains unclear. Using the TAU-P301L transgenic zebrafish line, we investigated how early Tau-induced neurotoxicity modifies BDNF signaling. Alterations in BDNF expression levels were observed as early as 48 h post fertilization in TAU-P301L zebrafish embryos while TrkB expression was not modified. Decreasing BDNF expression, using a knockdown strategy in wild-type embryos to mimic Tau-associated decrease, did not modify receptor expression but promoted neurotoxicity as seen by axonal outgrowth shortening and neuronal cell death. Moreover, the TrkB antagonist ANA-12 reduced the length of axonal projections. Rescue experiments with exogenous BDNF partially corrected neuronal alterations in TAU-P301L by counteracting primary axonal growth impairment but without effect on apoptosis. Importantly, the axonal rescue was proved functionally effective in a behavioral test, at a similar level as obtained with the GSK3β inhibitor LiCl, used as positive control. Finally, treatment with a TrkB agonist, 7,8-dihydroxyflavone, gave comparable results and allowed full rescue of locomotor response. We provided here strong evidences that Tau neurotoxicity provoked alterations in BDNF system and that BDNF pathway might represent an efficient therapeutic target.

Key words: BDNF signaling, TrkB, Tauopathies, TAU-P301L mutation, Zebrafish

Running title: BDNF signaling in tauopathies

1. Introduction

Intra-neuronal inclusions of hyperphosphorylated Tau aggregates, called neurofibrillary tangles (NFTs), are a distinctive neuropathological hallmark of tauopathies, *i.e.*, neurodegenerative diseases that include Alzheimer's disease (AD) and frontotemporal dementia (FTD) [1,2]. In AD patients, the development of NFTs strongly correlates with the severity of cognitive impairment as reflected by the Braak stages [3–5]. Under abnormal hyperphosphorylation, Tau proteins, which belong to the Microtubule-Associated Protein (MAP) family, become unstable and detach, forming Tau oligomers that are highly toxic species. Tau phosphorylation levels depend on a dynamic regulation by several kinases and phosphatases [6–8].

During neurodegenerative processes, neurotrophic support is markedly altered. Among neurotrophins, brain-derived neurotrophic factor (BDNF) plays pleiotropic roles in neuronal differentiation, survival, synaptic plasticity and memory consolidation during brain development and adult life. BDNF neuroprotective effects is essentially mediated by its high-affinity TrkB receptor [9–11]. A correlation has been established between decline in BDNF signaling and the level of cognitive impairment in AD [12,13]. Expression defects occur both at the protein and mRNA levels in blood and tissues of AD patients, as well as in mouse models. In a transgenic mouse model of AD that expresses human amyloid protein precursor (APP) and mutated Tau, cognitive impairment and synaptic loss could be rescued by BDNF treatment. Such results strongly supported a major role for BDNF in the etiology of the disease [14,15]. Moreover, recent findings uncover that BDNF deprivation triggers Tau proteolytic cleavage by activating delta-secretase, resulting in a Tau fragment that binds TrkB receptors and blocks its neurotrophic signals [16].

Although decreased BDNF/TrkB signaling and β-amyloid pathology development have been extensively studied, few reports have investigated BDNF alterations in primary tauopathies, such as frontotemporal dementia or Pick's disease. A decrease in BDNF expression was observed in brain tissues from patients with these tauopathies [17]. Several convergent recent data established that abnormal Tau expression (wild-type or mutated) led to BDNF expression deficiency [18–21]. A link between BDNF and Tau phosphorylation status was established in an *in vitro* study where BDNF treatment induced Tau dephosphorylation in differentiated neurons from mouse embryos [22], but this

was not confirmed *in vivo* [19]. However, the question of how tauopathy can affect BDNF signaling remains to be clarified.

Expression of human TAU-P301L mutation has been extensively used to generate transgenic animal models of tauopathy [23–25]. This missense mutation (proline to leucine) within the C-terminal microtubule-binding domain of the MAPT gene (codon 301, exon 10), reduces Tau affinity for microtubules and renders it more prone to abnormal hyper-phosphorylation [8,26,27].

In this study, we investigated the alterations of BDNF signaling in the early events of tauopathy-induced neurotoxicity using the TAU-P301L zebrafish transgenic line [28–30]. During zebrafish genome evolution, neurotrophin signaling was conserved and receptors duplicated. Hence, *bdnf*, *trk2a* and *trk2b* genes have been identified and exhibit a conserved expression within the central nervous system, consistent with the conservation of their neuronal roles throughout vertebrate evolution [31–34]. Therefore, zebrafish is considered as a valuable model to analyze BDNF signaling.

Our findings showed that tauopathy-related neurotoxicity is associated with alterations of BDNF signaling. We observed down-regulations of BDNF expression, but not TrkB, in TAU-P301L larvae. These observations suggested an impact on BDNF system in the very first steps of hyperphosphorylated Tau-induced neurotoxicity. Moreover, either BDNF knockdown or a pharmacological treatment with the TrkB receptor antagonist ANA-12 resulted in alterations of primary axonal growth. In addition, a treatment with exogenous BDNF in TAU-P301L larvae was sufficient to rescue primary axonal outgrowth and motility, but not neuronal apoptosis. Moreover, we demonstrated that treatment with the TrkB agonist 7,8-dihydroxyflavone lead to the similar rescue at the locomotor level. Therefore, analysis of the mechanisms by which BDNF rescue neuritic outgrowth and motility uncovered BDNF-TrkB signaling as necessary and sufficient to restore functional motorneuron properties in a Zebrafish model of Tauopathy.

2. Materials and Methods

2.1 Zebrafish maintenance

The present study was done according the recommendations of INSERM, Montpellier University and the European Convention for the Protection of Animals used for Experimental and Scientific Purposes. Zebrafish (*Danio rerio*) were maintained according to standard procedures [35]. Embryos were obtained from natural spawning and incubated in a water tank at 28°C. The Tg(elavI3.2:Gal4-VP16); Tg(UAS:hsaMAPT[P301L]:DsRed) transgenic line (TAU-P301L) was established as previously described (Paquet et al., 2009). The human hTAU-P301L mutation is expressed under the Huc promoter, which allows specific expression of the human MAPT gene in zebrafish neurons. Embryos were staged and maintained according to standard protocols. In parallel, the Tg(elavI3.2:Gal4-VP16);Tg(UAS:DsRed) transgenic line was also used as a Gal4-VP16 control line [29,36]. Control embryos were obtained either from Tg(elavI3.2:Gal4-VP16) x AB crossed line and were negative for DsRed expression (called siblings), or Tg(elavI3.2:Gal4-VP16); Tg(UAS:DsRed) x AB crossed line (called controls), genetic background was therefore identical for the two groups of embryos.

2.2 RNA extraction and cDNA synthesis

Total RNA was extracted from the whole zebrafish embryos at 48 hours post fertilization (hpf) using NucleoSpin R 8/96 RNA kit (Macherey-Nagel, Germany) according to manufacturer's instructions. RNA concentration and quality were evaluated with Agilent RNA 6000 Nano Kit (Agilent Technologies, Waldbronn, Germany). cDNA synthesis was performed as described previously [14].

2.3 Quantitative Real-Time PCR

Real-time PCR was performed using LightCycler 480 Instrument (RocheDiagnostics, Mannheim, Germany) according to manufacturer's instructions. PCR reactions were performed in a final volume of 6 μl with LC-DNA Master SYBR Green I mix, 1 μM of each primer and 1/25 diluted cDNA mixture for all genes added as PCR template (water was used as negative control). Amplification conditions were: (i) cDNA denaturation (1 cycle: 95°C for 10 min); (ii) amplification (45 cycles: denaturation 95°C

for 10 s, annealing 60°C for 10 s, elongation 72°C for 10 s); (iii) melting curve analysis (one cycle from 65°C to 95°C for 60 s); (iv) cooling (one cycle: 40°C for 60 s). Real-time detection of SYBR Green I fluorescence intensity, indicating the amount of PCR product formed, was measured at the end of each elongation phase. Threshold cycles for each target gene in control and TAU-P301L embryos were determined by using a housekeeping gene, actin, as normalization control. Primer sequences are indicated in supplementary material in Table S2.

2.4 Morpholino design and injection

At the one-cell stage, 3 ng of the following morpholinos (0.5 mM) were injected as described previously [37]. BDNF morpholinos (Gene Tools) are targeting the start codon since *bdnf* gene contains only one coding exon, no splice–targeted morpholino could be designed. The sequences used were:

MO1: 5′- CCAGTCGTAAAGGAGACCATTCAGC-3

MO2: 5'- CTAACCTGTTGGAACTTTACTGTCC- 3'

and a 5-base-mismatch from MO1, MM: 5′-CCACTCGAAAACGAGAGCATTGAGC-3

Since both morpholinos gave the same results in pilot experiments, results presented here were obtained using MO1. Morpholinos were injected in all embryos from TAU-P301L X AB cross, and morphants were screened at 24 and 48 hpf for DsRed fluorescence, injections were therefore performed blindly regarding TAUP301L expression.

2.5 Specificity of the antibodies

In order to ascertain the specificity of TrkB and BDNF polyclonal antibodies (#sc-12 and #sc-546 respectively, Santa Cruz Biotechnologies), we performed protein incubation with the mix of antibody and blocking peptide and verified the disappearance of the expected band (Fig. S1). In addition for BDNF/proBDNF detection, using morpholino knockdown, we observed the decrease of specific bands with several antibodies (Santa-Cruz polyclonal sc-546 and monoclonal sc-65513 antibodies, BDNF#1 mAb from Developmental Studies Hybridoma bank) [38]. Finaly, the anti proBDNF (sc-65513) had been already published for expression study of zebrafish BDNF [39]. TrkB polyclonal antibody (SC-12, Santa Cruz Biotechnologies) had been previously validated [31], but we also performed protein

6

incubation with the mix of antibody and blocking peptide and verified the disappearance of the expected band (Fig. S1).

2.6 Immunoblotting

For western blotting, 10 dechorionated and deyolked embryos [40] were homogenized in Laemmli sample buffer with protease and phosphatase inhibitors coktail (Roche, France). Lysates containing equivalent amounts of proteins (20 µg) derived from zebrafish embryos were resolved on 7% or 10% SDS-PAGE gels for TrkB or BDNF detection, respectively, and transferred to nitrocellulose membranes (Millipore). Antibody incubation was performed as previously described with one of the following primary antibodies [37]: BDNF (1:250, sc-546, Santa Cruz Biotechnologies), TrkB (1:250, sc-12, Santa Cruz Biotechnologies), actin was used as a loading control (1:2000, Sigma Aldrich). After primary antibody incubation, membranes were washed and incubated 1 h with horseradish peroxidase conjugated secondary antibodies: either anti-mouse IgG antibody (1:1000, Sigma Aldrich) or anti-rabbit IgG antibody (1:1000, Sigma Aldrich) depending on the primary antibody source. Signal detection was obtained as described and proteins bands were quantified using ImageJ v1.45 (NIH, Bethesda, MD, USA) densitometry analysis. [37]. Relative expression of experimental groups was obtained by normalizing to hTAU-P301L negative sibling group (Sib).

2.7 Neuronal primary cell culture of zebrafish

We followed the protocol developed by Chen et al. (2013) for spinal neuron culture. After chorion removal, 30 or 48 hpf control or TAU-P301L embryos were dissected and dissociated in culture medium (Leibovitz medium L15) supplemented with 2% FCS as described [41]. Cell suspension was passed through a 100 µm filter and placed at 28°C in incubator for 24 h, and the next day, primary cultures were fixed in PFA 4% and processed for immunofluorescence.

2.8 Immunofluorescence and quantification

For whole-mount antibody staining, larvae were anesthetized by immersion in 0.2 mg/mL MS222, fixed in 4% paraformaldehyde (PFA) and processed as previously reported [37,42]. Immunohistochemistry

was performed according to standard protocols, using mouse anti-acetylated tubulin (dilution 1:500, Sigma Aldrich), rabbit anti cleaved-caspase 3 (dilution 1:300, Thermo Scientific), rabbit anti-S202 antibody (dilution 1:300, Cell Signaling), rabbit anti-Tau PHF13 antibody (dilution 1:300, Cell Signaling), and a secondary Cy5-conjugated (dilution 1:800, Jackson Labs) or Alexa 488-conjugated antibodies (dilution 1:800, Molecular Probes). The samples were observed under confocal microscopy (Zeiss LSM 510, Leica SPE). Image stacks were processed and quantified with ImageJ. For each group, 10 embryos were analyzed. For axonal outgrowth quantification, 10 axonal extensions per embryo were measured using NeuronJ plugin (Image J). For cell death quantification, all the cleaved-caspase3 positive cells were counted in a constant field (665 x 665 μm^2), and 3 fields per embryo were recorded.

2.9 Exogenous BDNF treatment

Larvae at 5 hpf (50% epiboly) were incubated with human recombinant BDNF protein (Alomone) dissolved in water and diluted at 100 ng/ml in embryo medium after chorion opening as previously described [43]. Treatment was applied blindly for 48 hpf and then TAU-P301L larvae were sorted using DsRed fluorescence and tested for locomotion capacities or fixed before immunofluorescence labeling.

2.9 TrkB antagonist and agonist treatment

All embryos from TAU-P301L crosses were treated from 5 hpf with the TrkB antagonist ANA-12 or agonist 7,8-dihydroxyflavone (7,8-DHF) at 20 µM (Sigma Aldrich) or dimethylsulfoxide (DMSO, vehicle 0.01%) directly in the water and up to 48 hpf or 5 dpf. Larvae were screened at 24 and 48 hpf for DsRed fluorescence, treatment with ANA-12, 7,8-DHF or DMSO was therefore performed blindly, independently of TAU-P301L expression. Three different spawns were treated and after DsRed screening, larvae were analyzed for locomotor activities (n = 150).

2.10 Behavioral analysis

Touch-evoked escape response (TR) assay was performed on larvae at 3 and 5 dpf. Larvae were first acclimatized on a stereoscope for 15 min at 28 °C. Tactile stimulus was applied to the tail of the larvae

by a gentle touch with a micropipette tip. The escape behaviour was recorded and was scored according to the distance swum immediately after the stimulus [44].

The motility was tested with two distinct protocols using the Zebrabox tracking system (Zebralab®, Viewpoint, Lissieu, France). First, 4 dpf larvae (with or without BDNF treatment) were placed in 24-well plate in obscurity and locomotion was recorded under infrared light during two periods of 10 min, separated by 10 min without recording. The second test assessed the visual motor response (VMR) at 5 days with the following light/dark alternation protocol: 30 min habituation with light off, then 3 repetitions of a cycle with light on during 15 min and light off during 15 min. Four dpf larvae were placed in 96-well plate after the BDNF treatment and the experiment performed at 5 dpf. For each protocol, the swum distance was analyzed per bin of 90 sec and compared between groups.

2.11 Statistical Analysis

Data are presented as mean ± SEM. All statistical analyses were done using Prism 5.0 software (GraphPad Software Inc). Statistical significance between groups was determined by unpaired Student's *t*-test or non-parametric Mann-Whitney *t*-test due to small experimental groups. P value < 0.05 was considered as statistically significant. Each western blot experiment was repeated at least 4 times (n ≥ 4). Behavioral VMR results were analyzed using two-way ANOVA followed by a *post-hoc* Tukey's test.

3. Results

3.1 Overexpression of human TAU-P301L down-regulates BDNF protein levels in zebrafish

To determine whether BDNF signaling could be altered by over-expression of mutated hTau, we took advantage of the zebrafish TAU-P301L line in which hyperphosphorylated Tau induced neuronal defects as early as 48 h [29]. We first investigated BDNF and its receptor expression at the protein level at the end of the embryonic developmental phase, *i.e.*, 48 hpf using TAU-P301L-DsRed negative siblings as controls. Receptor genes *ntrk* are duplicated in zebrafish while *bdnf* gene remains unique. Sequence homologies with human and mice proteins range from 70% for *bdnf* to 50% for *ntrk* genes that should allow antibodies cross-reactivity. To assess specificity of the antibodies, we used different strategies. First, for BDNF/proBDNF detection, we performed transient knockdown using morpholino (see below) and observed the decrease of specific bands with several antibodies, some of them were already published for expression study of BDNF in zebrafish [33,38]. We then assessed both pro-BDNF and mature BDNF expression in TAU-P301L line. Pro-BDNF was detected at 25-29 kDa and mature BDNF at 14-17 kDa (Figs. 1A, 1B). TAU-P301L embryos display a significant decrease of pro-BDNF (-39%, $p < 0.05$) and mature BDNF levels (-55%, $p < 0.05$) compared to control TAU negative siblings (Figs. 1A, 1B). Second, BDNF receptor expression was analyzed using antibodies raised against mouse (TrkB) proteins. For TrkB detection, we performed protein incubation with the mix of antibody and blocking peptide, and verified the disappearance of the expected band (Fig. S1). In addition, this TrkB polyclonal antibody had been previously validated [31] and gave the expected band size. Since neither zebrafish Ntrk2a nor Ntrk2 could be dissociated, we then kept the same designation as TrkB (thus corresponding to Ntrk2a and Ntrk2b) in all western blot experiments. In TAU-P301L embryos, TrkB protein levels were comparable to control values (+13%, $p > 0.05$; Figs. 1C, 1D).

Alteration of mRNA levels was also investigated using RT-qPCR and we compared *bdnf*, *ntrk2a*, *ntrk2b* mRNA levels in TAU-P301L embryos and control siblings (Table S2). Normalization to either *actin* or *ef1* gene expressions gave similar results (data not shown). mRNA levels for the 3 tested genes were not significantly different between the two groups at 48 hpf (Fig. S2).

Next, we evaluated the expression of BDNF and its receptor at the cellular level, using primary neuron culture from 48 hpf embryos. Due to some expression heterogeneity in hTAU-P301L, we took

advantage of DsRed expression, either in hTAU-P301L or in the Huc-Gal4-UAS-DsRed embryos and focus only on DsRed-positive neurons. In control DsRed-positive neurons, we observed a strong expression of BDNF and TrkB in cell bodies as well as in neurites (Fig. 1D). In TAU-P301L neurons, fluorescence signals was lower for BDNF and, particularly, neuritic outgrowth was often not or very faintly labeled (pointed by arrows; Fig. 1E) while TrkB expression was comparable to control at the cell body and neuritic levels. These observations confirmed previous western blot results.

In summary, the data showed that overexpression of the human TAU-P301L mutation in zebrafish neurons induced a marked decrease of BDNF expression as early as 48 hpf, while no modification of TrkB levels was observed.

3.2 TAU-P301L- induced early neuronal cell death is independent of BDNF decrease

In order to further investigate the relationship between BDNF and neuronal toxicity, we performed BDNF knockdown in control sibling embryos (Sib) and assessed receptor expression levels. The knockdown strategy of BDNF levels using morpholinos (MO) was favored against a knockout mutant in order to reach for a large number of embryos a knockdown level about 50%, thus matching the levels in TAU-P301L. We did not observed major anatomical alterations of the zebrafish embryos after MO injection. Two specific morpholinos for BDNF were tested and gave similar results (see Material and Methods). A mismatch morpholino control (MM) gave comparable results as non-injected embryos (data not shown). We first assessed the extent of BDNF knockdown in control Gal4-UAS-DsRed embryos by quantifying the reduction of pro- and mature BDNF proteins. We detected reductions of -59% ($p < 0.05$) and -56% ($p < 0.05$) for pro-BDNF and mature BDNF, respectively, in morphants (Sib-MO) compared to mismatch control (Sib-MM) (Figs. 2A, 2B). In these conditions, the quantification of TrkB expression levels in Sib-MO revealed no significant differences for TrkB levels compared to MM controls albeit a trend towards higher TrkB levels was observed (Figs. 2C, 2D). These results indicated that BDNF knockdown can represent an independent control to compare with Tau condition.

We next address neuronal phenotypes in both conditions BDNF KD and Tau line. As established by previous reports, TAU-P301L mutation is associated with neuronal loss [29,45]. To define whether BDNF signaling reduction might be involved in neuronal apoptosis, we investigated the consequences

of a BDNF knockdown, in the range level of the TAU-P301L reduction, on neuronal integrity. Cell death was examined in Sib-MM or BDNF Sib-MO at 48 hpf. We observed a slight and significant increase in neuronal immunolabeling of cleaved-caspase-3 in Sib-MO compared with control Sib-MM ($p < 0.05$; Figs. 3A, 3B). By contrast, cell death analysis in TAU-P301L embryos revealed a major apoptosis at 48 hpf, significantly higher than observed in Sib-MO ($p < 0.001$; Fig. 3C). These observations suggested that the decrease in BDNF signaling is not responsible for the marked apoptosis observed in hTAU-P301L embryos. In order to ascertain the role of BDNF in hTAU-P301L context, rescue experiments were performed by incubating exogenous BDNF [43]. BDNF treatment was applied as early as 50% of epiboly (5-6 hpf) and maintained up to 48 hpf. This led to a complete rescue of cell death in BDNF-treated Sib-MO (Fig. 3B), validating our BDNF delivery approach. However, no significant decrease of neuronal death was observed in TAU-P301L after BDNF treatment (Fig. 3C). Altogether, our results indicated that BDNF decrease in TAU-P301L was not responsible for neuronal apoptosis and suggested other deleterious factors in addition to BDNF depletion.

3.3 Rescue of TAU-P301L axonal phenotype by BDNF

Associated with neurodegeneration, impairment of axonal outgrowth is considered as a hallmark of tauopathy (Almeida et al., 2016; Paquet et al., 2009) and is observed in TAU-P301L embryos. We measured neurite length, using acetylated neuronal tubulin immunostaining (Fig. 4). To standardize our analysis, only the first five outgrowing caudal primary motoneurons anterior to the end of the yolk extension were examined. Compared to Sib-MM controls, TAU-P301L embryos display shortened axonal length at 48 hpf (-44%; Figs. 4A, 4B, 4F), as previously reported (Giustiniani et al., 2014; Paquet et al., 2009). Interestingly, the decrease was similar to that observed after BDNF knockdown, in Sib-MO embryos (- 45% compared to 100% control) (Figs. 4D, 4F). Exogenous BDNF treatment induced a partial but very significant attenuation of axonal growth deficit in BDNF-treated TAU-P301L embryos (-30%; Figs. 4C, 4F), as well as in BDNF-treated Sib-MO embryos (69%; Figs. 4E, 4F), confirming that the BDNF decrease observed in TAU-P301L embryos could be responsible for the axonal deficits.

To further demonstrate BDNF signaling involvement in this process, we blocked TrkB receptor using ANA-12 [47]. Axonal growth was measured at 48 hpf after treatments of control or TAU-P301L

embryos with 20 µM ANA-12 or DMSO as vehicle. We observed a significant decrease of axonal development in ANA-12-treated control sibling (Sib+ANA) embryos (-43%, $p < 0.001$; Figs. 5A, 5B, 5E). DMSO-treated TAU-P301L embryos also showed a significant reduction in axonal length (-38%, $p < 0.001$; Figs. 5C, 5E), that was of similar extent as Sib+ANA larvae. Interestingly, ANA-12 treatment of TAU-P301L embryos led to a further reduction of axonal length as compared to DMSO-treated TAU-P301L embryos (-50% compared to -38%, $p < 0.05$; Figs. 5D, 5E), suggesting that BDNF signaling through TrkB was still operational.

Altogether, these results highlighted that BDNF/TrkB signaling was reduced in TAU-P301L embryos and more importantly that it could be rescued upon exogenous BDNF treatment.

3.4 Functional recovery of TAUP301L larvae after BDNF or agonist treatments

In order to assess a functional impact of the neuritic outgrowth, we first analyzed the motility and locomotor behavior of TAU-P301L at 3 and 5 dpf with the Touch-evoked Response (TR) test. A marked defective locomotor behavior was observed at 3 dpf and to a lesser extend also at 5 dpf consistent with previous data at 2 dpf ($p < 0.05$; Figs. 6A, 6B). We next analyzed the locomotor activity through tracking recording at 4 dpf and observed a decrease in swimming distance consistent with the touch-evoked response phenotype (Figs 6A-C). Next, we asked if a rescue could be induced by BDNF treatment in TAU-P301L larvae at 4 dpf. We observed a recovery of the TAU-P301L larvae motility following BDNF treatment that appeared not significantly different from controls, albeit at the limit of significance ($p = 0.054$; Fig. 6B). Our results however suggested that a specific BDNF deficit could be involved in axonal tract atrophy and motility deficit linked to TAU-P301L expression.

The motor behavior functions were also investigated through the visual motor reflex (VMR) at 5 dpf. Light alternation induced startle responses at the light transition, *i.e.*, a decrease in activity during the ON phases and a stimulation of activity during the OFF phase. Activity changes were measured as the total distance travelled during each session (Fig. 6D). TAU-P301L larvae showed higher responses compared with control siblings, during both ON or OFF sessions (Figs. 6D). Such differences might reflect defect in movement coordination and/or over-reactivity at the light stimuli (Fig. 6D). As Paquet et al. (2009) previously showed some efficacy of GSK3β inhibitors in the same zebrafish line [29], we

tested LiCl. A 5 mM LiCl treatment, from 24 hpf until 5 dpf, allowed a complete rescue of the VMR response of TAU-P301L larvae (Figs. 6D, 6E).

BDNF (100 nM) was applied using the same protocol and completely abolished the increased VMR reaction and the motility profile of BDNF-treated TAU-P301L larvae was similar to control ($p < 0.001$; Figs. 6F, 6G). Furthermore, a treatment with 20 µM 7,8-DHF, a TrkB agonist, also restored the VMR responses during the OFF sessions, with absence of high bursts of activity for TAU-P301L larvae, consistent with a functional TrkB activity (Fig. 6H).

4. Discussion

BDNF plays a well-established neuroprotective role. *In vitro* studies as well as *in vivo* knockdown models showed that BDNF can modulate AD severity or Tau phosphorylation level [12,22]. Reports investigating the role of BDNF and its receptor on Tau–induced neurotoxicity *in vivo* led to some result discrepancies that might be linked to transgene construct that target specific neuronal subpopulation, such THY, Prion or Calcium/Calmodulin dependent kinase II alpha (CaMKII) promoters [48–50]. It may also rely on the mutation studied, P301L versus P301S. In the present study, we took advantage of the zebrafish model to combine transgenic and pharmacological approaches, in the TAU-P301L line where P301L mutation is driven under the pan-neuronal promoter HuC, and analyzed the role of variations in BDNF and TrkB expression levels.

In the TAU-P301L line, we observed marked reductions of BDNF and proBDNF, which are consistent with previous reports in patients with various types of tauopathies [17]. Data from mouse models, including for instance the P301L mouse model, revealed imbalance between proBDNF and BDNF levels [19,51]. A recent report also showed a down-regulation of BDNF in cellular and animal models after human Tau overexpression [21]. However, these data diverged from previous work showing that BDNF was not downregulated in hippocampal neurons from THY-Tau22 transgenic mice [52] or that stable BDNF levels were associated with increased TrkB expression in the retina of TAU-P301S transgenic mice [20]. Such differences might reflect organ specificities. Indeed, several studies have now established such Tau-induced BDNF down-regulation [17,19,21]. These discrepancies highlighted the importance to clarify the relationship between Tau and BDNF using *in vivo* models. We therefore focused on the early steps of neurotoxicity linked to Tau hyperphosphorylation, in an attempt to decipher the primary Tau-dependent toxic mechanisms.

Regarding BDNF receptor expression, we investigated the high affinity receptor TrkB, which binds preferentially mature BDNF, and we observed that TrkB levels were unchanged in TAU-P301L larvae and therefore represented a potential therapeutic target. A link between Tau hyperphosphorylation and disruption of microtubule trafficking and BDNF axonal transport has been recently described [53]. This is in line with the absence of a neuritic localization of BDNF in TAU-P301L zebrafish neurons. As

Tau neurotoxicity progressed, it led to neuronal cell death and shortening of axonal outgrowth. We here described the involvement of BDNF in neuronal cell death and shortening of axonal outgrowth, by using pharmacological TrkB blocking, BDNF knockdown and rescue experiments. First, BDNF knockdown in control larvae resulted in low neuronal cell death that was rescued by exogenous BDNF application. In TAU-P301L larvae, a major apoptosis occurred that was not rescued by exogenous BDNF, suggesting that TAU-P301L neurotoxicity is independent of BDNF reduction. Second, BDNF knockdown resulted in 55-60% decrease in proBDNF and BDNF levels that led to an axonal outgrowth reduction comparable to TAU-P301L. Moreover, we were able to restore partially this TAU-P301L phenotype with recombinant BDNF treatment. Axonal shortening was alleviated. In order to address receptor function, TrkB inhibition was induced using the antagonist ANA-12 and a comparable axonal defect was observed.

Furthermore, at the behavioral level, analysis of the touch-evoked response not only confirmed an alteration at 3 and 5 dpf, but it also showed that TAU-P301L mutation in zebrafish resulted in a characteristic VMR: during dark phases, TAU-P301L larvae showed a hyperactive response at 5 dpf. A similar hyperactivity and agitative-like behavior was observed with the rTg4510 mice expressing TAU-P301L mutation driven by the CaMKII promoter [54]. In addition, this hyper-reactivity to the light stimulus was abolished using LiCl treatment. This observation was consistent with data obtained in rodent models and patients [55,56]. Actually, a recent open label clinical trial in Alzheimer's disease patients showed that a low dose of lithium may represent an effective treatment for agitation symptoms. Interestingly, the behavioral improvement under lithium was associated with increased BDNF serum levels [56]. In our model, recombinant BDNF treatment led to functional recovery, in the VMR test, similarly as observed with lithium. In addition, the TrkB agonist 7,8-DHF treatment also completely rescued the locomotor phenotype of TAU-P301L larvae. The protective efficacy of 7,8-DHF in AD models was recently demonstrated, since the drug improved spatial memory in Tg2576 mice [57] and prevented $A\beta$ deposition in 5XFAD AD mice, inhibiting the pathological cleavage of APP and Tau [58].

We showed that BDNF downregulation is an early event linked to Tau-induced neurotoxicity and our findings strongly suggested that BDNF/TrkB signaling reduction contributed to a primary defect

responsible for the axonal phenotype observed in TAU-P301L zebrafish. TrkB signaling was still efficient and could restore BDNF function during axonal and synaptic plasticity development. Further studies are needed to explore the molecular mechanisms of the rescue process, however the striking motility and locomotor behavior recovery was promising for long-term benefit of BDNF or TrkB agonist treatment, and a protective role on later stages with progressive cell death. Such data are consistent with BDNF protective function against Tau-induced neurotoxicity recently reported in mice through effective cognitive repair and protection against neuronal loss [19]. Numerous strategies are aiming at producing selective TrkB agonists or BDNF-mimetic peptides [58] but alternative BDNF-stimulating pharmacological treatment could also be proposed. For instance, sigma-1 receptor agonists increase BDNF levels [59–61] and presently in clinical trials in AD, Huntington's disease or amyotrophic lateral sclerosis. Our results confirmed the potentialities of developing new strategies aiming to alleviate BDNF decrement in Tauopathies and AD, which could be rapidly tested in the zebrafish model.

5. Acknowledgments

Funding

Authors contributions

CB, AY, MS, NC, MR: Conceptualization, Methodology and experiments design

CB, AY, MS : performed the experiments and analyzed the data, CB, AY, MR: Writing- Original draft preparation. JMV, MR: Supervision. JMV, TM, MR: Writing- Reviewing and Editing.

6. Disclosure statement

The authors declare no financial or competing interests.

7. References

[1]   M.G. Spillantini, M. Goedert, Tau pathology and neurodegeneration, Lancet Neurol. 12 (2013) 609–622. https://doi.org/10.1016/S1474-4422(13)70090-5.

[2]   D.R. Williams, Tauopathies: classification and clinical update on neurodegenerative diseases associated with microtubule-associated protein tau, Intern Med J. 36 (2006) 652–660. https://doi.org/10.1111/j.1445-5994.2006.01153.x.

[3]   P.V. Arriagada, J.H. Growdon, E.T. Hedley-Whyte, B.T. Hyman, Neurofibrillary tangles but not senile plaques parallel duration and severity of Alzheimer's disease, Neurology. 42 (1992) 631–639.

[4]   R.J. Bateman, C. Xiong, T.L.S. Benzinger, A.M. Fagan, A. Goate, N.C. Fox, D.S. Marcus, N.J. Cairns, X. Xie, T.M. Blazey, D.M. Holtzman, A. Santacruz, V. Buckles, A. Oliver, K. Moulder, P.S. Aisen, B. Ghetti, W.E. Klunk, E. McDade, R.N. Martins, C.L. Masters, R. Mayeux, J.M. Ringman, M.N. Rossor, P.R. Schofield, R.A. Sperling, S. Salloway, J.C. Morris, Dominantly Inherited Alzheimer Network, Clinical and biomarker changes in dominantly inherited Alzheimer's disease, N. Engl. J. Med. 367 (2012) 795–804. https://doi.org/10.1056/NEJMoa1202753.

[5]   H. Braak, E. Braak, Neuropathological stageing of Alzheimer-related changes, Acta Neuropathol. 82 (1991) 239–259.

[6]   F. Hernandez, J.J. Lucas, J. Avila, GSK3 and tau: two convergence points in Alzheimer's disease, J. Alzheimers Dis. 33 Suppl 1 (2013) S141-144. https://doi.org/10.3233/JAD-2012-129025.

[7]   X.-H. Liu, Z. Geng, J. Yan, T. Li, Q. Chen, Q.-Y. Zhang, Z.-Y. Chen, Blocking GSK3β-mediated dynamin1 phosphorylation enhances BDNF-dependent TrkB endocytosis and the protective effects of BDNF in neuronal and mouse models of Alzheimer's disease, Neurobiol. Dis. 74 (2015) 377–391. https://doi.org/10.1016/j.nbd.2014.11.020.

[8]   M. von Bergen, S. Barghorn, L. Li, A. Marx, J. Biernat, E.M. Mandelkow, E. Mandelkow, Mutations of tau protein in frontotemporal dementia promote aggregation of paired helical filaments by enhancing local beta-structure, J. Biol. Chem. 276 (2001) 48165–48174. https://doi.org/10.1074/jbc.M105196200.

[9]   J. Lu, Y. Xu, W. Hu, Y. Gao, X. Ni, H. Sheng, Y. Liu, Exercise ameliorates depression-like behavior and increases hippocampal BDNF level in ovariectomized rats, Neurosci. Lett. 573 (2014) 13–18. https://doi.org/10.1016/j.neulet.2014.04.053.

[10]   T. Numakawa, S. Suzuki, E. Kumamaru, N. Adachi, M. Richards, H. Kunugi, BDNF function and intracellular signaling in neurons, Histol. Histopathol. 25 (2010) 237–258.

[11]   W.J. Tyler, M. Alonso, C.R. Bramham, L.D. Pozzo-Miller, From acquisition to consolidation: on the role of brain-derived neurotrophic factor signaling in hippocampal-dependent learning, Learn. Mem. 9 (2002) 224–237. https://doi.org/10.1101/lm.51202.

[12]   S. Peng, J. Wuu, E.J. Mufson, M. Fahnestock, Precursor form of brain-derived neurotrophic factor and mature brain-derived neurotrophic factor are decreased in the pre-clinical stages of Alzheimer's disease, J. Neurochem. 93 (2005) 1412–1421. https://doi.org/10.1111/j.1471-4159.2005.03135.x.

[13]   S. Peng, D.J. Garzon, M. Marchese, W. Klein, S.D. Ginsberg, B.M. Francis, H.T.J. Mount, E.J. Mufson, A. Salehi, M. Fahnestock, Decreased brain-derived neurotrophic factor

depends on amyloid aggregation state in transgenic mouse models of Alzheimer's disease, J. Neurosci. 29 (2009) 9321–9329. https://doi.org/10.1523/JNEUROSCI.4736-08.2009.

[14]   S. Arancibia, M. Silhol, F. Moulière, J. Meffre, I. Höllinger, T. Maurice, L. Tapia-Arancibia, Protective effect of BDNF against beta-amyloid induced neurotoxicity in vitro and in vivo in rats, Neurobiol. Dis. 31 (2008) 316–326. https://doi.org/10.1016/j.nbd.2008.05.012.

[15]   A.H. Nagahara, D.A. Merrill, G. Coppola, S. Tsukada, B.E. Schroeder, G.M. Shaked, L. Wang, A. Blesch, A. Kim, J.M. Conner, E. Rockenstein, M.V. Chao, E.H. Koo, D. Geschwind, E. Masliah, A.A. Chiba, M.H. Tuszynski, Neuroprotective effects of brain-derived neurotrophic factor in rodent and primate models of Alzheimer's disease, Nat Med. 15 (2009) 331–337. https://doi.org/10.1038/nm.1912.

[16]   J. Xiang, Z.-H. Wang, E.H. Ahn, X. Liu, S.-P. Yu, F.P. Manfredsson, I.M. Sandoval, G. Ju, S. Wu, K. Ye, Delta-secretase-cleaved Tau antagonizes TrkB neurotrophic signalings, mediating Alzheimer's disease pathologies, Proc. Natl. Acad. Sci. U. S. A. 116 (2019) 9094–9102. https://doi.org/10.1073/pnas.1901348116.

[17]   J.C. Belrose, R. Masoudi, B. Michalski, M. Fahnestock, Increased pro-nerve growth factor and decreased brain-derived neurotrophic factor in non-Alzheimer's disease tauopathies, Neurobiol. Aging. 35 (2014) 926–933. https://doi.org/10.1016/j.neurobiolaging.2013.08.029.

[18]   İ.L. Atasoy, E. Dursun, D. Gezen-Ak, D. Metin-Armağan, M. Öztürk, S. Yılmazer, Both secreted and the cellular levels of BDNF attenuated due to tau hyperphosphorylation in primary cultures of cortical neurons, Journal of Chemical Neuroanatomy. 80 (2017) 19–26. https://doi.org/10.1016/j.jchemneu.2016.11.007.

[19]   S.-S. Jiao, L.-L. Shen, C. Zhu, X.-L. Bu, Y.-H. Liu, C.-H. Liu, X.-Q. Yao, L.-L. Zhang, H.-D. Zhou, D.G. Walker, J. Tan, J. Götz, X.-F. Zhou, Y.-J. Wang, Brain-derived neurotrophic factor protects against tau-related neurodegeneration of Alzheimer's disease, Transl Psychiatry. 6 (2016) e907. https://doi.org/10.1038/tp.2016.186.

[20]   N. Mazzaro, E. Barini, M.G. Spillantini, M. Goedert, P. Medini, L. Gasparini, Tau-Driven Neuronal and Neurotrophic Dysfunction in a Mouse Model of Early Tauopathy, J. Neurosci. 36 (2016) 2086–2100. https://doi.org/10.1523/JNEUROSCI.0774-15.2016.

[21]   E. Rosa, S. Mahendram, Y.D. Ke, L.M. Ittner, S.D. Ginsberg, M. Fahnestock, Tau downregulates BDNF expression in animal and cellular models of Alzheimer's disease, Neurobiology of Aging. 48 (2016) 135–142. https://doi.org/10.1016/j.neurobiolaging.2016.08.020.

[22]   E. Elliott, R. Atlas, A. Lange, I. Ginzburg, Brain-derived neurotrophic factor induces a rapid dephosphorylation of tau protein through a PI-3Kinase signalling mechanism, European Journal of Neuroscience. 22 (2005) 1081–1089. https://doi.org/10.1111/j.1460-9568.2005.04290.x.

[23]   Q. Bai, E.A. Burton, Zebrafish models of Tauopathy, Biochim. Biophys. Acta. 1812 (2011) 353–363. https://doi.org/10.1016/j.bbadis.2010.09.004.

[24]   J. Götz, Y.-A. Lim, Y.D. Ke, A. Eckert, L.M. Ittner, Dissecting toxicity of tau and beta-amyloid, Neurodegener Dis. 7 (2010) 10–12. https://doi.org/10.1159/000283475.

[25]   M. Higuchi, B. Zhang, M.S. Forman, Y. Yoshiyama, J.Q. Trojanowski, V.M.-Y. Lee, Axonal degeneration induced by targeted expression of mutant human tau in oligodendrocytes of transgenic mice that model glial tauopathies, J. Neurosci. 25 (2005) 9434–9443.

https://doi.org/10.1523/JNEUROSCI.2691-05.2005.

[26]   S. Barghorn, Q. Zheng-Fischhöfer, M. Ackmann, J. Biernat, M. von Bergen, E.M. Mandelkow, E. Mandelkow, Structure, microtubule interactions, and paired helical filament aggregation by tau mutants of frontotemporal dementias, Biochemistry. 39 (2000) 11714–11721.

[27]   D. Fischer, M.D. Mukrasch, M. von Bergen, A. Klos-Witkowska, J. Biernat, C. Griesinger, E. Mandelkow, M. Zweckstetter, Structural and microtubule binding properties of tau mutants of frontotemporal dementias, Biochemistry. 46 (2007) 2574–2582. https://doi.org/10.1021/bi061318s.

[28]   J. Giustiniani, B. Chambraud, E. Sardin, O. Dounane, K. Guillemeau, H. Nakatani, D. Paquet, A. Kamah, I. Landrieu, G. Lippens, E.-E. Baulieu, M. Tawk, Immunophilin FKBP52 induces Tau-P301L filamentous assembly in vitro and modulates its activity in a model of tauopathy, Proc. Natl. Acad. Sci. U.S.A. 111 (2014) 4584–4589. https://doi.org/10.1073/pnas.1402645111.

[29]   D. Paquet, R. Bhat, A. Sydow, E.-M. Mandelkow, S. Berg, S. Hellberg, J. Fälting, M. Distel, R.W. Köster, B. Schmid, C. Haass, A zebrafish model of tauopathy allows in vivo imaging of neuronal cell death and drug evaluation, J. Clin. Invest. 119 (2009) 1382–1395. https://doi.org/10.1172/JCI37537.

[30]   J.E. Sepulveda-Diaz, S.M. Alavi Naini, M.B. Huynh, M.O. Ouidja, C. Yanicostas, S. Chantepie, J. Villares, F. Lamari, E. Jospin, T.H. van Kuppevelt, A.G. Mensah-Nyagan, R. Raisman-Vozari, N. Soussi-Yanicostas, D. Papy-Garcia, HS3ST2 expression is critical for the abnormal phosphorylation of tau in Alzheimer's disease-related tau pathology, Brain. 138 (2015) 1339–1354. https://doi.org/10.1093/brain/awv056.

[31]   F. Abbate, M.C. Guerrera, G. Montalbano, M.B. Levanti, G.P. Germanà, M. Navarra, R. Laurà, J.A. Vega, E. Ciriaco, A. Germanà, Expression and anatomical distribution of TrkB in the encephalon of the adult zebrafish (Danio rerio), Neurosci. Lett. 563 (2014) 66–69. https://doi.org/10.1016/j.neulet.2014.01.031.

[32]   E. De Felice, I. Porreca, E. Alleva, P. De Girolamo, C. Ambrosino, E. Ciriaco, A. Germanà, P. Sordino, Localization of BDNF expression in the developing brain of zebrafish, J. Anat. 224 (2014) 564–574. https://doi.org/10.1111/joa.12168.

[33]   A. Germanà, C. Sánchez-Ramos, M.C. Guerrera, M.G. Calavia, M. Navarro, R. Zichichi, O. García-Suárez, P. Pérez-Piñera, J.A. Vega, Expression and cell localization of brain-derived neurotrophic factor and TrkB during zebrafish retinal development, J. Anat. 217 (2010) 214–222. https://doi.org/10.1111/j.1469-7580.2010.01268.x.

[34]   F. Hallböök, K. Wilson, M. Thorndyke, R.P. Olinski, Formation and evolution of the chordate neurotrophin and Trk receptor genes, Brain Behav. Evol. 68 (2006) 133–144. https://doi.org/10.1159/000094083.

[35]   M.C. Fishman, D.Y. Stainier, R.E. Breitbart, M. Westerfield, Zebrafish: genetic and embryological methods in a transparent vertebrate embryo, Methods Cell Biol. 52 (1997) 67–82.

[36]   E. Ogura, Y. Okuda, H. Kondoh, Y. Kamachi, Adaptation of GAL4 activators for GAL4 enhancer trapping in zebrafish, Dev. Dyn. 238 (2009) 641–655. https://doi.org/10.1002/dvdy.21863.

[37]   S. Huc-Brandt, N. Hieu, T. Imberdis, N. Cubedo, M. Silhol, P.L.A. Leighton, T.

Domaschke, W.T. Allison, V. Perrier, M. Rossel, Zebrafish prion protein PrP2 controls collective migration process during lateral line sensory system development, PLoS ONE. 9 (2014) e113331. https://doi.org/10.1371/journal.pone.0113331.

[38]   A. Jimenez-Gonzalez, A. García-Concejo, S. López-Benito, V. Gonzalez-Nunez, J.C. Arévalo, R.E. Rodriguez, Role of morphine, miR-212/132 and mu opioid receptor in the regulation of Bdnf in zebrafish embryos, Biochim. Biophys. Acta. 1860 (2016) 1308–1316. https://doi.org/10.1016/j.bbagen.2016.03.001.

[39]   A. Germanà, R. Laurà, G. Montalbano, M.C. Guerrera, V. Amato, R. Zichichi, S. Campo, E. Ciriaco, J.A. Vega, Expression of brain-derived neurotrophic factor and TrkB in the lateral line system of zebrafish during development, Cell. Mol. Neurobiol. 30 (2010) 787–793. https://doi.org/10.1007/s10571-010-9506-z.

[40]   V. Link, A. Shevchenko, C.-P. Heisenberg, Proteomics of early zebrafish embryos, BMC Dev. Biol. 6 (2006) 1. https://doi.org/10.1186/1471-213X-6-1.

[41]   Z. Chen, H. Lee, S.J. Henle, T.R. Cheever, S.C. Ekker, J.R. Henley, Primary neuron culture for nerve growth and axon guidance studies in zebrafish (Danio rerio), PLoS ONE. 8 (2013) e57539. https://doi.org/10.1371/journal.pone.0057539.

[42]   N. Cubedo, E. Cerdan, D. Sapede, M. Rossel, CXCR4 and CXCR7 cooperate during tangential migration of facial motoneurons, Mol. Cell. Neurosci. 40 (2009) 474–484.

[43]   H. Diekmann, O. Anichtchik, A. Fleming, M. Futter, P. Goldsmith, A. Roach, D.C. Rubinsztein, Decreased BDNF levels are a major contributor to the embryonic phenotype of huntingtin knockdown zebrafish, J. Neurosci. 29 (2009) 1343–1349. https://doi.org/10.1523/JNEUROSCI.6039-08.2009.

[44]   C.B. Kimmel, J. Patterson, R.O. Kimmel, The development and behavioral characteristics of the startle response in the zebra fish, Developmental Psychobiology. 7 (1974) 47–60. https://doi.org/10.1002/dev.420070109.

[45]   B. Frost, J. Götz, M.B. Feany, Connecting the dots between tau dysfunction and neurodegeneration, Trends Cell Biol. 25 (2015) 46–53. https://doi.org/10.1016/j.tcb.2014.07.005.

[46]   M.F. Almeida, R.S. Chaves, C.M. Silva, J.C.S. Chaves, K.P. Melo, M.F.R. Ferrari, BDNF trafficking and signaling impairment during early neurodegeneration is prevented by moderate physical activity, IBRO Reports. 1 (2016) 19–31. https://doi.org/10.1016/j.ibror.2016.08.001.

[47]   S. Chakravarty, S. Maitra, R.G. Reddy, T. Das, P. Jhelum, S. Kootar, W.D. Rajan, A. Samanta, R. Samineni, S. Pabbaraja, S.G. Kernie, G. Mehta, A. Kumar, A novel natural product inspired scaffold with robust neurotrophic, neurogenic and neuroprotective action, Sci Rep. 5 (2015) 14134. https://doi.org/10.1038/srep14134.

[48]   J. Lewis, E. McGowan, J. Rockwood, H. Melrose, P. Nacharaju, M. Van Slegtenhorst, K. Gwinn-Hardy, M. Paul Murphy, M. Baker, X. Yu, K. Duff, J. Hardy, A. Corral, W.L. Lin, S.H. Yen, D.W. Dickson, P. Davies, M. Hutton, Neurofibrillary tangles, amyotrophy and progressive motor disturbance in mice expressing mutant (P301L) tau protein, Nat. Genet. 25 (2000) 402–405. https://doi.org/10.1038/78078.

[49]   K. Santacruz, J. Lewis, T. Spires, J. Paulson, L. Kotilinek, M. Ingelsson, A. Guimaraes, M. DeTure, M. Ramsden, E. McGowan, C. Forster, M. Yue, J. Orne, C. Janus, A. Mariash, M. Kuskowski, B. Hyman, M. Hutton, K.H. Ashe, Tau suppression in a

neurodegenerative mouse model improves memory function, Science. 309 (2005) 476–481. https://doi.org/10.1126/science.1113694.

[50]   K. Schindowski, A. Bretteville, K. Leroy, S. Bégard, J.-P. Brion, M. Hamdane, L. Buée, Alzheimer's disease-like tau neuropathology leads to memory deficits and loss of functional synapses in a novel mutated tau transgenic mouse without any motor deficits, Am. J. Pathol. 169 (2006) 599–616. https://doi.org/10.2353/ajpath.2006.060002.

[51] N. Deters, L.M. Ittner, J. Götz, Divergent phosphorylation pattern of tau in P301L tau transgenic mice, European Journal of Neuroscience. 28 (2008) 137–147. https://doi.org/10.1111/j.1460-9568.2008.06318.x.

[52]   S. Burnouf, K. Belarbi, L. Troquier, M. Derisbourg, D. Demeyer, A. Leboucher, C. Laurent, M. Hamdane, L. Buee, D. Blum, Hippocampal BDNF expression in a tau transgenic mouse model, Curr Alzheimer Res. 9 (2012) 406–410.

[53]   M. Le, A. M Weissmiller, L. Monte, P.H. Lin, T. Hexom, O. Natera, C. Wu, R. Rissman, Functional Impact of Corticotropin-Releasing Factor Exposure on Tau Phosphorylation and Axon Transport, PloS One. 11 (2016) e0147250. https://doi.org/10.1371/journal.pone.0147250.

[54]   P. Jul, C. Volbracht, I.E.M. de Jong, L. Helboe, A.B. Elvang, J.T. Pedersen, Hyperactivity with Agitative-Like Behavior in a Mouse Tauopathy Model, J. Alzheimers Dis. 49 (2016) 783–795. https://doi.org/10.3233/JAD-150292.

[55]   D.P. Devanand, J.G. Strickler, E.D. Huey, E. Crocco, B.P. Forester, M.M. Husain, I.V. Vahia, H. Andrews, M.M. Wall, G.H. Pelton, Lithium Treatment for Agitation in Alzheimer's disease (Lit-AD): Clinical rationale and study design, Contemp Clin Trials. 71 (2018) 33–39. https://doi.org/10.1016/j.cct.2018.05.019.

[56]   G. Griebel, J. Stemmelin, M. Lopez-Grancha, D. Boulay, G. Boquet, F. Slowinski, P. Pichat, S. Beeské, S. Tanaka, A. Mori, M. Fujimura, J. Eguchi, The selective GSK3 inhibitor, SAR502250, displays neuroprotective activity and attenuates behavioral impairments in models of neuropsychiatric symptoms of Alzheimer's disease in rodents, Sci Rep. 9 (2019) 18045. https://doi.org/10.1038/s41598-019-54557-5.

[57]   L. Gao, M. Tian, H.-Y. Zhao, Q.-Q. Xu, Y.-M. Huang, Q.-C. Si, Q. Tian, Q.-M. Wu, X.-M. Hu, L.-B. Sun, S.M. McClintock, Y. Zeng, TrkB activation by 7, 8-dihydroxyflavone increases synapse AMPA subunits and ameliorates spatial memory deficits in a mouse model of Alzheimer's disease, J. Neurochem. 136 (2016) 620–636. https://doi.org/10.1111/jnc.13432.

[58]   C. Chen, Z. Wang, Z. Zhang, X. Liu, S.S. Kang, Y. Zhang, K. Ye, The prodrug of 7,8-dihydroxyflavone development and therapeutic efficacy for treating Alzheimer's disease, Proc. Natl. Acad. Sci. U.S.A. 115 (2018) 578–583. https://doi.org/10.1073/pnas.1718683115.

[59]   C.R. Eddings, N. Arbez, S. Akimov, M. Geva, M.R. Hayden, C.A. Ross, Pridopidine protects neurons from mutant-huntingtin toxicity via the sigma-1 receptor, Neurobiol. Dis. 129 (2019) 118–129. https://doi.org/10.1016/j.nbd.2019.05.009.

[60]   M. Fujimoto, T. Hayashi, R. Urfer, S. Mita, T.-P. Su, Sigma-1 receptor chaperones regulate the secretion of brain-derived neurotrophic factor, Synapse. 66 (2012) 630–639. https://doi.org/10.1002/syn.21549.

[61]   K. Kikuchi-Utsumi, T. Nakaki, Chronic treatment with a selective ligand for the sigma-1 receptor chaperone, SA4503, up-regulates BDNF protein levels in the rat hippocampus, Neurosci. Lett. 440 (2008) 19–22. https://doi.org/10.1016/j.neulet.2008.05.055.

8. Figure legends

Figure 1. BDNF and p75NTR expression are down-regulated in transgenic TAU-P301L zebrafish embryos. Western blot analyses of: (A) pro-BDNF, (B) mature BDNF (BDNF), (C) TrkB levels in control (Sib) and TAU-P301L embryos at 48 hpf. Typical blots are shown above quantifications. Quantifications of the relative intensities were normalized to actin level (loading control) and sibling levels (Sib) was set at 100% (dotted line). N = 5-8 per group, # p < 0.05, Mann-Whitney's test. (D-E) BDNF and p75NTR expression decrease at the neuronal level. Immunofluorescent staining of BDNF, p75NTR and TrkB on primary neural cell cultures obtained from embryos from (D) control HucGal4-VP16-UAS-DsRed line, and (E) the TAU-P301L line. In (D) DsRed expression was used to assess neuronal identity. Strong expressions of BDNF or receptors were observed at the cell body as well as the neuritic levels. In (E) DsRed expression identified neurons that expressed human TAUP301L mutation (arrows). Cell body exhibited lower levels of BDNF and p75NTR while TrkB expression was similar to control neurons in (D) (boxes). In addition, p75NTR expression in neuritis was dramatically reduced (dotted boxes). Scale bar = 50 µm.

Figure 2. BDNF knockdown did not modify receptor expressions. Western blot analyses of: (A) pro-BDNF, (B) mature BDNF (BDNF), (C) TrkB and (D) p75NTR protein levels in control embryos injected with mismatch morpholino (Sib-MM) and siblings injected with BDNF morpholino (Sib-MO). Typical blots are shown above quantifications and include TAU-P301L sample at 48 hpf, for visual comparison of the relative intensities. Quantifications were normalized to actin level (loading control) and Sib-MM level was set at 100% (dotted line). N = 4-8 per group, # p < 0.05, Mann-Whitney's test.

Figure 3. BDNF knockdown induced early neuronal cell death. (A) Apoptosis detection (insert: neuronal extension level considered) using cleaved-caspase 3 immunostaining (c-caspase 3, cyan) at 48 hpf in control siblings (Sib-MM), sibling-MO (Sib-MO), TAU-P301L (DsRed[+]) and TAU-P301L with BDNF treatment (P301L+BDNF, DsRed[+]). Dotted lines defined embryo nervous system. (B) Quantitative analysis of labeled cells at 48 hpf shows a significant increase of apoptosis in Sib-MO compared to control, and a complete rescue after BDNF treatment. (C) Quantitative analysis of labeled

cells at 48 hpf shows a marked increase of apoptosis TAU-P301L compared to Sib-MM controls, unaffected by the BDNF treatment. N = 24-29 per group, * $p < 0.05$, *** $p < 0.001$, Mann-Whitney's test.

Figure 4. Defects in primary axonal growth in TAU-P301L embryos associated with BDNF decrease. Immunostaining with acetylated neuronal tubulin antibody revealed motorneuron axonal tracts in 48 hpf larvae: (A) control Sib-MM, (B) TAU-P301L, (C) TAU-P301L treated with BDNF, (D) siblings morphant larvae Sib-MO, and (E) Sib-MO treated with BDNF. (F) Quantitative analysis of axonal length using reconstruction in NeuronJ and normalization relative to Sib-MM controls. Note that axonal tracts are shortened and disorganized in (B) and (D) and that exogenous BDNF treatment partially rescued axonal outgrowth in (C) and (E). N = 24 per group in (F), ## $p < 0.01$.

Figure 5. TrkB antagonist treatment led to neuritic growth impairment. (A) Immunostaining with acetylated neuronal tubulin antibody revealed motorneuron axonal tracts in 48 hpf embryos: (A) DMSO-treated control siblings (Sib-DMSO), (B) ANA-12-treated (Sib+ANA), (C) TAU-P301L (TAUP301L+ANA), and (D) TAU-P301L treated with BDNF (TAUP301L+BDNF). (E) Quantification of axonal lengths using NeuronJ plugin (ImageJ). N = 12 per group, # $p < 0.05$ vs. Sib+DMSO, * $p < 0.05$ vs. TAUP301L+DMSO, unpaired t test.

Figure 6. Behavioral responses of treated larvae: (A) Touch response at 3 dpf and (B) Tracking of locomotor activity measured at 4 dpf with typical trajectories of control siblings, TAUP301L and BDNF-treated TAUP301L larvae and (C) quantification of total distance. (D-H)Visual motor response (VMR) measured at 5 dpf: (D, F) ON/OFF sessions were applied as 15/15 min cycles, represented by the black/white bar. (E, G, H) Average of the total distance moved every 90 sec bin was plotted for each groups. (D, E) VMR representative profil of 5 dpf siblings and TAU-P301L larvae after treatment with LiCl. (F, G) VMR representative profil of 5 dpf siblings and TAU-P301L larvae after treatment with BDNF (100 nM) or (H) 7,8-DHF (20 μM). Three independent experiments were performed, n = 24 per group. # $p < 0.05$, ## $p < 0.01$, Mann-Whitney's test.

Figure 1

Figure2

A

kDa   Sib-MM   Sib-MO   TAU-P301L

25-29   proBDNF

45   Actin

B

kDa   Sib-MM   Sib-MO   TAU-P301L

14   BDNF

45   Actin

C

kDa   Sib-MM   Sib-MO   TAU-P301L

145   TrkB

45   Actin

Figure 3

A

c-caspase 3

Sib-MM

Sib-MO

DsRed

c-caspase 3

merge

TAU-P301L

TAU-P301L+BDNF

B

C

Figure 4

Sib-MM A

TAUP301L B

TAUP301L + BDNF C

Sib-MO D

Sib-MO + BDNF E

F

% axonal length/ control

##

##

Sib-MM | TAU-P301L | TAU-P301L +BDNF | Sib-MO | Sib-MO +BDNF

Figure 5

Figure 6

A Touch response 3 and 5 dpf

distance (cm) — 3d tau-, 3dtau+, 5dtau-, 5dtau+

B Sib, TAU-P301L, TAU-P301L +BDNF

Total distance (mm) — BDNF-, BDNF+ — Sib, TAU-P301L — #

C light cycles

total distance / bin (90sec) vs time (sec)
— Sib
— Sib +LiCl
— TAU-P301L +LiCl
— TAU-P301L

total distance (mm) / control — LiCl -, LiCl + — Sib, TAU-P301L

D light cycles

total distance / bin (90sec) vs time (sec)
----- Sib
— Sib +BDNF
— TAU-P301L +BDNF
— TAU-P301L

E total distance / control — BDNF-, BDNF+ — Sib, TAU-P301L

distance totale (cm) / control — DHF -, DHF + — Sib, TAU-P301L

Gene	Sequence
bdnf	F GCAACCAAGTGCCTTTGGAG R TGTCCGGCATTGCGAGTTAT
ntrk2b	F GCCAGATCGAGGCTACATC R TGATCCACGTCAGGTATACG
ntrk2a	F GACGCGGAGCGCAGTATTA R GTAGTTTCGGGTTGCTCTGGA
ngfra	F CATGAGAATGCAGACGCCCT R GGTTTCATCCCGACACTCCT
ngfrb	F AGAGTGCTGCAAACAATGCC R GAAGAAGCCGTAGTCGCAGA
EF-1 alpha	F TTCTGTTACCTGGCAAAGGG R TTCAGTTTGTCCAACACCCA
actin (actb1)	F TGTGAGTTTTCAGTGCACGC R TGGGCCTCATCTCCCACATA

Table S1. Primer sequencs for qPCR expression analysis

Fig. S1: Specificity of antibodies: binding inhibition with the blocking peptide
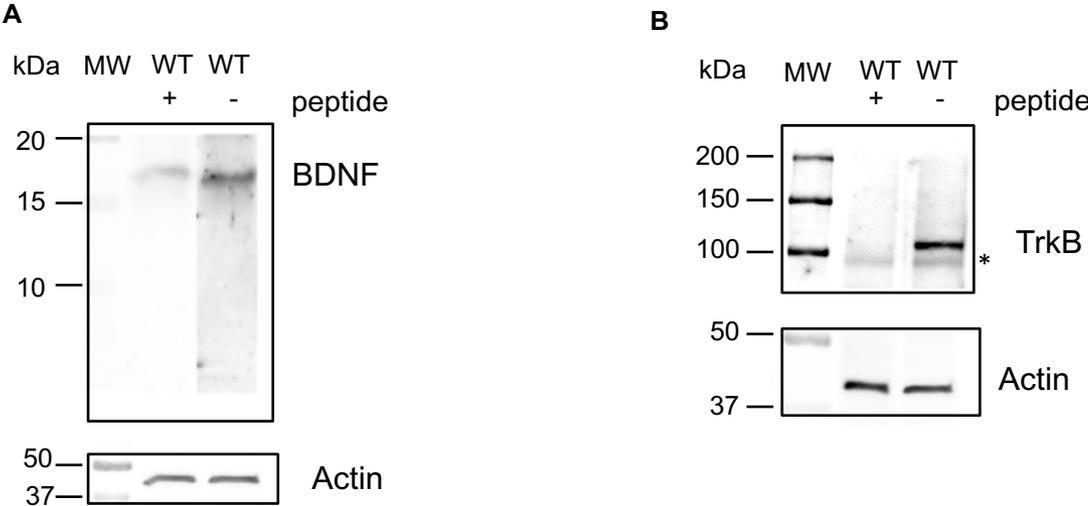
Figure Sup 1. Specificity antibody test
(A) Incubation of BDNF (sc-546, Santa Cruz Biotechnologies) with blocking peptide results in the loss of signal.
(B) Incubation of TrkB (SC-12, Santa Cruz Biotechnologies) antibodies with blocking peptide results in the loss of signal.
* non specific signal

Fig. S2

A

B
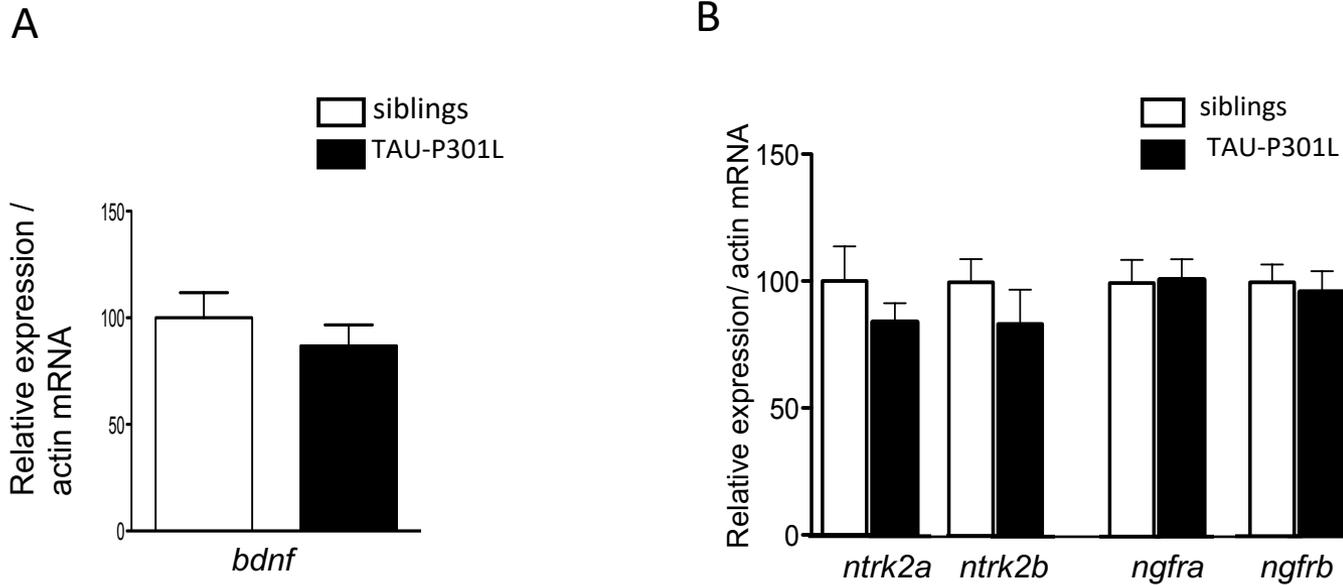
Figure Sup 2. qPCR levels of bdnf and its receptors in TAU-P301L
(A) qPCR analysis shows the relative *bdnf* gene expression levels in control (siblings) and TAU-P301L embryos at 48 hpf. Values were normalized to the expression of *actin* and expressed as the mean±s.e.m of four independent experiments. No significant differences were observed.
(B) qPCR analysis shows the relative *ntrkb2a,ntrkb2b, ngfra* and *ngfrb* gene expression levels in control and TAU-P301L embryos at 48 hpf. Values were normalized to the expression of *actin* and expressed as the mean±s.e.m of four independent experiments